Mestrado Integrado em Medicina Dentária

Faculdade de Medicina da Universidade de Coimbra

Micromovimentos com diferentes tipos de conexões entre o pilar protético e o implante.

Micromovements with different type of connections between the implant and the abutment.

Eduardo Manuel Rodrigues Portela

Orientador: Professor Doutor Fernando Guerra

Co-Orientador: Dr. Salomão Rocha

Coimbra, 2013

Micromovimentos com diferentes tipos de conexões entre o pilar protético e o implante.

Micromovements with different type of connections between the implant and the abutment.

Portela E, Guerra F, Rocha S

Department of Dentistry, Faculty of Medicine, University of Coimbra
Av. Bissaya Barreto, Blocos de Celas
3000-075 Coimbra
Portugal

E-mail: eduardo.r.portela@hotmail.com

Abstract: Introduction: The type of implant-abutment connection can influence the micromovements of those components during function. Conical internal connections have been referred in the literature as the most stable. However, a previous study using MIS® conical connection titanium abutments presented the highest values of micromovements. The purpose of this study is to compare the micromovements of these abutments with anti-rotational and rotational internal conical connections using three dimensional Digital Image Correlation (DIC 3D). **Materials and Methods:** 10 Mis® Titanium abutments (5 rotational and 5 anti-rotational) were screwed at 30N to C1® Implants (Mis®, Tel-Aviv, Israel) mounted in acrylic and loaded at a 30º angle to 200N in a universal testing machine (AG-I Shimadzu®). Micromovements were collected under load with a non-contact measuring system Vic-3D (Correlated Solutions, Inc). Data was statistically analyzed using mixed-ANOVA procedures and independent samples t-tests. **Results**: No statistically significant interactions were found between the abutment type and load intensity on displacement. No differences were found between the rotational and anti-rotational abutments. **Conclusion**: Rotational and anti-rotational MIS® internal conical connection abutments performed in the same range of micromovements assuring a predictable clinical use.

Resumo: Introdução: O tipo de conexão implante/pilar pode influenciar os micromovimentos das reabilitações em função. A literatura tem referido as conexões cónicas internas como as mais estáveis. No entanto, num estudo anterior, pilares de titânio Mis® com conexão cónica interna apresentaram os maiores valores de micromovimentos. O objetivo deste estudo é avaliar os micromovimentos destes pilares com conexão cónica interna rotacional e anti-rotacional através do método de Correlação Imagem Digital 3D (CID 3D). **Materiais e Métodos**: 10 pilares Mis® Titanium (5 rotacionais e 5 anti-rotacionais) foram aparafusados a 30N a implantes C1® (Mis®, Tel-Aviv, Israel) montados em acrílico e submetidos com angulação de 30º a 200N de carga em máquina de testes universal (AG-I Shimadzu®). Os micromovimentos foram recolhidos sob carga usando um método sem contacto de correlação de imagem Vic-3D (Correlated Solutions, Inc). Os dados foram analisados usando os testes de mixed-ANOVA e teste de t para amostras independentes. **Resultados:** Não foram encontradas interações estatisticamente significativas entre entre o tipo de pilar, a carga e os micromovimentos obtidos. Não foram encontradas diferenças entre os dois tipos de pilares. **Conclusão**: Os pilares MIS® rotacionais e anti-rotationais de conexão cónica interna apresentam intervalos similares de valores de micromovimentos assegurando boa previsibilidade na utilização clínica.

1. Introduction

Implant dentistry is a valid and predictable treatment option for the rehabilitation of partially and completely edentulous arches. More than 30 years of evidence involving the clinical use of endosseous implants have shown excellent long-term results[1].

Most implant systems consist of two components: the endosteal part (the implant), which is placed in a first surgical phase, and the transmucosal connection (the abutment), which is typically attached after successful implant osseointegration to support the prosthetic restoration[2].

For the long-term success of implant-supported restorations, crestal bone stability and healthy soft tissues are considered necessary. If these 2 parameters are accomplished, implant therapy can be a reliable treatment with an impressive outcome[3-4]. However, biological and particularly technical complications are frequent[5].

While postsurgical bone height around implant systems is somewhat predictable, its preservation is subject to both mechanical[6-13] and microbiological[14-21] aspects of the implant–abutment connection[22-23].

Having said that one of the most important parameters related to bone loss around dental implants is the implant-abutment interface, in wich a microgap is present[24-25]. Some authors have suggested that the presence of this microgap could result in microbiologic colonization, causing an inflammatory response and, consequently, bone remodeling[24-33]. Authors have also suggested that micromovements at the implant-abutment interface are the determining factor in bone resorption[34-35].

Under loading, where the abutment components are subjected to eccentric forces, the number and size of gaps can be increased. Moreover, micromovements of implant components during function may instigate a pumping effect that facilitates bacterial leakage through the implant-abutment interface[36].

During the transmission of masticatory forces the lateral component of the force is thought to be responsible for creating bending moments on the implant-abutment interface. At the surface facing the external load, the implant and the abutment

experience tensile stress from bending, while on the opposite surface, the connection is subject to compression[37].

These forces can create a vibrating movement and cause the threads to “back off”. The backing off of the threads leads to a reduction in the effective preload and diminishes the ability of the screw to maintain the joint stability thereby increasing the implant-abutment interface gap space[38].

The relationship between the implant-abutment interface and the bone response has been extensively studied, and some reports have shown that different implant designs have variable effects on tissue response. These differences among the systems are due to variations in the connection geometry, materials, and overall screw mechanics. The implant-abutment connection stability is also influenced by factors such as component fit, machining accuracy, saliva contamination, and screw preload[6-8, 39-42].

With the purpose of studying this mechanical issue some measuring analytical techniques have been described in the literature for micromovements measurement and gap determination. These include scanning electron microscopy, travelling microscope, liquid strain gauges and digital image correlation[43-44].

Under these circumstances, alternative implant systems with different connections and materials have been hurled to the market and their aim is to preserve peri-implant soft and hard tissues.

Conical internal connections were developed to achieve a friction-based fit of the implant components[45-48] and it is reported in literature that this type of connection have the least values of micromovements[49].

The purpose of this study is to understand if there is a correlation between this micromovements and the use of a rotational or a non-rotational implant-abutment connection. In order to explain the unexpected results obtained in a previous study done in this university.

2. Materials and Methods

In this research study, Three Dimensional Digital Image Correlation (DIC 3D), was used to visualize and quantify micromovements of two different types of implant abutments connections for single crown restorations from the same manufacturer: Mis® Titanium conical connection standard cementing post (SP) with rotational and anti-rotational system for Implant C1 (Mis®, Tel-Aviv, Israel)

Table I – All materials summarized that are going to be tested.

Group	N	Abutment/Implant	Lot	Manufacturer	Connection type	Material
A	5	**C1 implant 4.20x13 mm**	REF:C1-13420	MIS®	Conical connection with an anti-rotational six position, cone index.	Titanium
		Conical Connection Standard Cementing post (**Anti-Rotational)**	REF:CS-MAC10			
B	5	**C1 implant 4.20x13 mm**	REF:C1-13420	MIS®	Conical connection with an anti-rotational six position, cone index.	Titanium
		Conical Connection Standard Cementing post (**Rotational)**	REF:CS-MAC10			

Abutments and Implants

In **Group A**: five Mis® titanium internal conical connection Standard Cementig post (n=5) with an anti-rotational cone index, with 12 mm of height, were applied on five C1 implants with a conical connection with a platform diameter of 4,20 mm and 13 mm of length, and tightened with a torque of 30 Ncm (Table 1).

In **Group B**: five Mis® titanium internal conical connection Standard Cementing post (n=5) with a rotational cone index, with 12 mm of height, were applied on five C1 implants with a conical connection with a platform diameter of 4,20 mm and 13mm of length, and tightened with a torque of 30 Ncm (Table 1).

Fig. I Implant C1 (Mis®, Tel-Aviv, Israel)

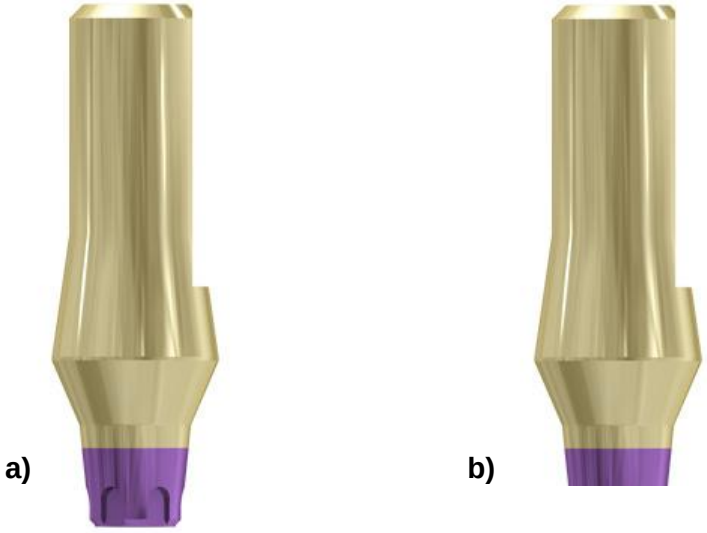

Fig. II Conical connection standard cementing posts
a) Group A – Anti-Rotational; **b)** Group B - Rotational

Preparation of the samples

The implants were embedded in a fast curing (7-8 minutes approximately at 22º), cold polymerising, three component resin, based on modified polyester (Technovit 4000 – Heraeus Kulzer, Wehrheim Germany). Technovit 4000 guaranteed that geometrically demanding samples are optimally embedded. Its excellent adhesion

properties with regard to metal are a guarantee of gapless embedding of all metal samples. This resin shows properties similar to bone elasticity.

The implants were incorporated in the resin, leaving about 3-4 mm of implant outside the resin surface using molds that allowed the implants to keep an angle of 0º relative to the vertical axis (Figure III).

Fig. III The molds obtained from the inclusion of the implants in the resin.

Loading Tests

The abutments were loaded at an angle of 30° to the vertical axis, this value was obtained according to the study of Morneburg et al. with a force of up to 200 N[50]. For this purpose a universal test-machine (AG-I Shimadzu®, Riverwood Drive, USA) was used, with a velocity established of 0,5mm/min until the maximum force was reached.

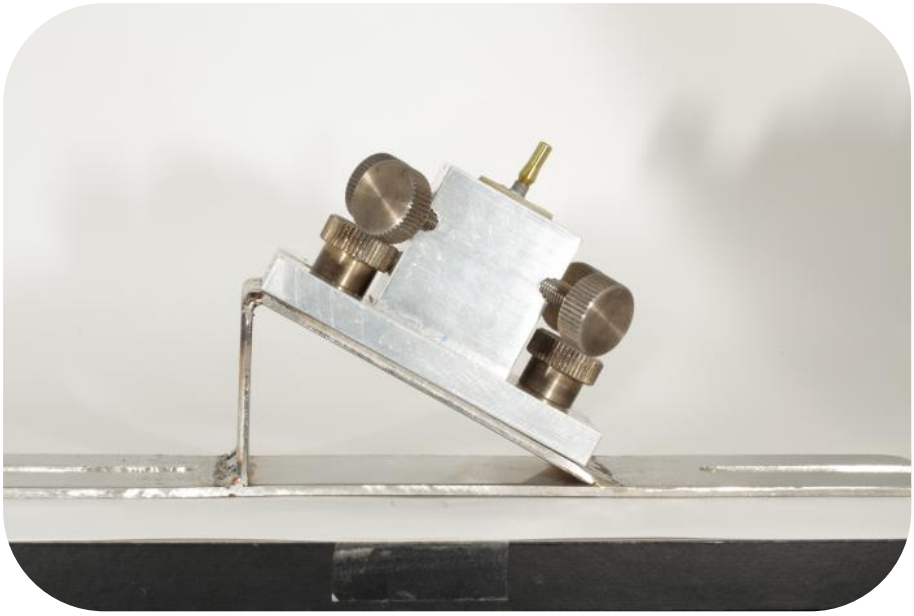

Fig. IV A sample inserted in the 30º angled support base.

The interface of the implant-abutment connection were examined and the micromovements measurements were performed by the optical method of 3D digital image correlation (DIC) with two high speed photographic cameras (Point Grey GRAS-20S4M-C, 1624x1224 pixels) which can capture images at a maximum frame rate of 19 fps (frames per second) and the video correlation system Vic-3D 2010 (Correlated Solutions®, Columbia, USA). The DIC 3D method is an optical measurement technique that can determine the three dimensional contour of small object's surfaces, obtaining displacement fields without contact and with high resolution. This system uses the digital image of two high speed photographic cameras (Point Grey GRAS-20S4M-C, 1624x1224 pixels) and the video correlation software (Vic-3D 2010) to track the surface displacement field of an object [51] (Figure V).

Digital Image Correlation

Digital image correlation (DIC) is a full-field image analysis method, based on grey value digital images, that allows determination of the contour and surface displacements of an object under load in three dimensions.

An algorithm defines a field of "subsets" on the object's surface using the digital images. These subsets are N by N pixel boxes that contain an array of pixel gray-scale

values. An advanced tracking algorithm can determine the translation, rotation and deformation of these subsets in loaded images with respect to a reference frame[51-52].

The high resolution of the deformation measurements in space and time can accurately set the absolute position and displacement of objects, even if they display high amplitudes and large rigid body movements[51]. Viewing from different positions at an object, two image sensors, offer enough information to perceive the object as three dimensional, comparable to human vision. Using a stereoscopic camera setup, each object point is focused on a specific pixel in the image plane of the respective camera[52].

Fig. V DIC 3D camera setup**.**

The position of each surface point in the two images can be identified, by applying a correlation algorithm using a stochastic intensity pattern on the object's surface. A matching accuracy of the original and the transformed surface of better than 0,01 pixel can be achieved, through this correlation algorithm. The stochastic pattern used was applied with a colored spray paint and cut in squares so that it could be pasted: one in the abutment and another in the implant (Figure VI)[51].

Fig. VI A sample being tested in the test-machine (AG-I Shimadzu) using a pointed tip.

Calibration

To begin the collection of images, calibration of the cameras was made and it was given a score to each calibration. This process is described as the process of determining the projection parameters (intrinsic and extrinsic imaging parameters). Simultaneously, images of a target with a known accurate pattern were recorded with both cameras and the system displays in real time the tracking of the target markers. Automatically the system acquired a sequence of images of the target positioned at different angles and from this sequence the projection parameter was calculated[51].

The quality of the measurement is directly related to the accuracy of the projection parameters. Typically eight images are sufficient to calculate all calibration parameters accurately[51].

Using the projection parameters of the system, the 3-dimensional coordinates for each object point can be calculated leading to a 3-dimensional contour of the object. Along the loading steps each camera followed the changes of the grey value pattern and the surface displacements of the object were calculated. A series of about 400 images corresponding to a time sequence of 0,08 seconds was evaluated. Each time the cameras were used there is an error of projection for each measurement and a limit was defined that indicate that a new calibration is needed[51].

Statistical Analyses

Statistical analysis was performed with IBM SPSSStatistics 20.0. Descriptive statistics were calculated for micromovements in U, V and W directions under dynamic loads of 50, 100, 150, 200N for each abutment type. Normality of the distributions was determined using Shapiro-Wilk test. A mixed ANOVA test was used to determine whether there were differences between the two groups under different loads and to estimate the effect of the type of abutment and load intensity on micromovements. Independent samples t-test was used to determine the mean difference between the micromovements of both groups. Significance level was set at $\alpha=0,05$.

3. Results

Maximum values of displacement for each sample were obtained from the dynamic behavior for all implant-abutment connections exposed to loads of 50, 100, 150, 200N, at angles of 30º relative to the implant axis and are reported at Table II - Appendix. Micromovements were detected in all implant-abutment connections used. For each loading condition, three types of movements in different directions were captured by DIC 3D system. According to recorded movements there were different values for:

U: the lateral movement, from left to right. When negative, it meant a movement of the object to the left;

V: referred to the occluso-cervical movement. When negative, it translated the deepening of the object occluso movement;

W: referred to the antero-posterior movement. When the values were negative it meant the posterior movement of the object.

Overview images were provided in figure VII exhibiting the details of the movements observed at the interface implant-abutment for a sample of group A, anti-rotational abutment.

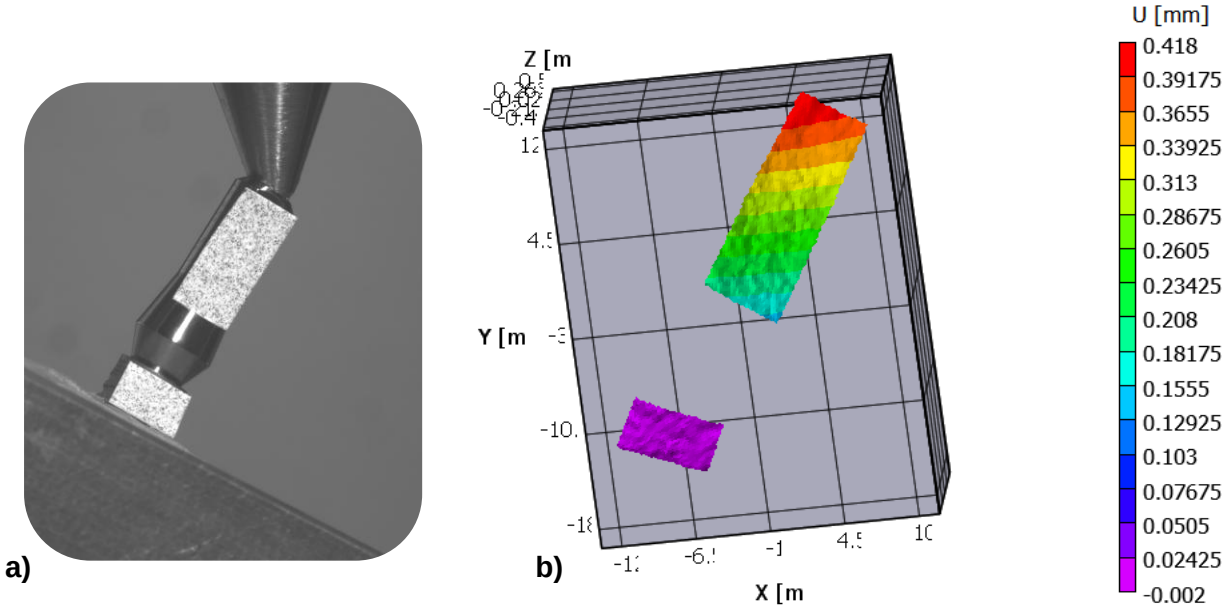

Fig. VII- a) A sample of an anti-rotational abutment being subjected to 200N; **b)** Graphic of the same sample obtained via 3D image correlation. The red region represents the higher values of micromovements in the U direction of the abutment relative to the implant (whose speckle pattern was considered for rigid body motion removal).

The descriptive statistics for the micromovements of the two groups subjected to different loads are summarized in table III. There were no outliers in the data, as shown by the Boxplots in Graphics 1 to 3 (Appendix).

Table III - Mean values and standard deviation obtained from the dynamic behavior for all implant-abutment connections exposed to maximum forces of 50, 100, 150, 200N, at angles of 30º relative to the implant axis. According to recorded movements there are different values for: **U**: it refers to the lateral movement, **V**: it refers to the occluso-cervical movement, **w**: it refers to the antero-posterior movement. **P.E**. – Mean Projection Error for each force loaded.

Group	**N**	**Implant System**	**Connection type**	**Torque**	**Calibration score**		Micro. in mm at **50N** (P.E.: 0,045)	Micro. in mm at **100N** (P.E.: 0,036)	Micro. in mm at **150N** (P.E.:0,036)	Micro. in mm at **200N** (P.E.:0,038)
A	5	MIS®	Anti-Rotational	30Ncm	0,047	u	**0,038** ±0,030	**0,095** ±0,059	**0,179** ±0,085	**0,265** ±0,108
						v	**-0,037** ±0,050	**-0,094** ±0,080	**-0,164** ±0,124	**-0,236** ±0,162
						w	**-0,001** ±0,069	**-0,009** ±0,080	**-0,005** ±0,081	**0,004** ±0,064
Group	**N**	**Implant System**	**Connection type**	**Torque**	**Calibration score**		Micro. in mm at **50N** (P.E.: 0,036)	Micro. in mm at **100N** (P.E.:0,050)	Micro. in mm at **150N** (P.E.:0,050)	Micro. in mm at **200N** (P.E.:0,058)
B	5	MIS®	Rotational	30Ncm	0,043	u	**0,068** ±0,045	**0,123** ±0,045	**0,179** ±0,045	**0,233** ±0,048
						v	**-0,022** ±0,039	**-0,052** ±0,047	**-0,090** ±0,043	**-0,124** ±0,044
						w	**-0,064** ±0,078	**-0,083** ±0,104	**-0,087** ±0,097	**-0,118** ±0,105

A mixed ANOVA test considering Greenhouse-Geisser correction for violation of sphericity assumption was performed to understand if there was an interaction between the abutment type and force applied on the micromovements along the medio-lateral, vertical and antero-posterior directions (U, V, W).

There was no statistically significant interaction between both the abutment type and load intensity on displacement along the U direction, F(1,075; 8,604)= 2,64, p = 0,14, partial η2 = 0,248. Similar results were obtained for V and W directions (F(1,048; 8,383)= 3,316, p=0,104, partial η2 = 0,293 and F(1,809; 14,474)= 3,563, p=0,059, partial η2 = 0,308, respectively). These results are illustrated in graphics 4a, 4b and 4c, representing the estimated marginal means of micromovements on the U, V and W directions for each group under load.

Graphic 4 – Profile plot for estimated marginal means of micromovements of anti-rotational and rotational abutments under loads of 50, 100, 150 and 200N: **a)** U direction; **b)** V direction; **c)** W direction.

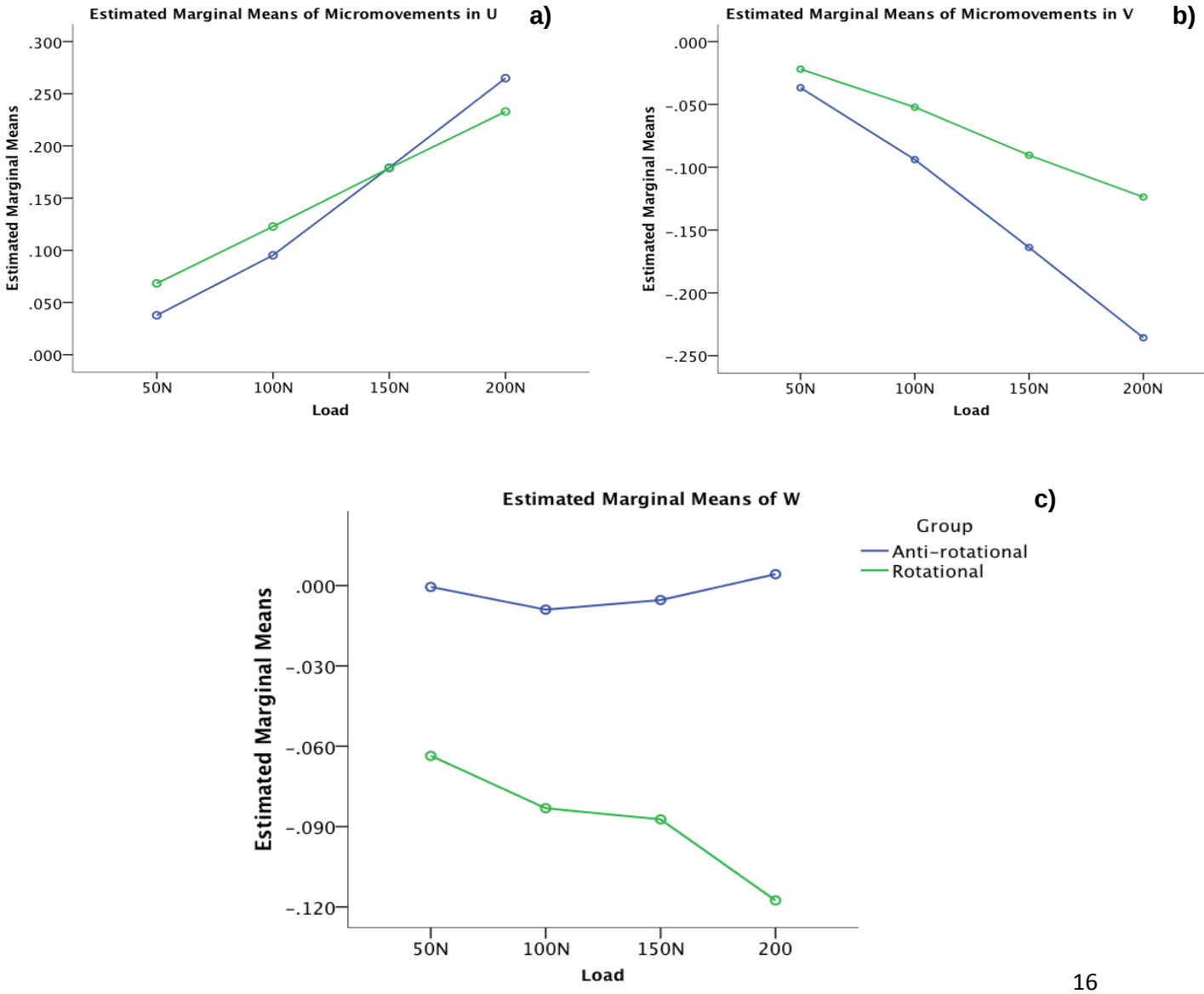

The type of abutment did not seem to be responsible for the variation of the micromovements, as shown in table IV for the between-subjects effects.

Table IV – Table of between–subjects effects determining the main effect of the type of connection for differences in micromovements regardless of force. df- degrees of freedom; F- ANOVA test value.

	df	F	p	Partial Eta Squared
U	1	0,030	0,866	0,004
V	1	1,463	0,261	0,155
W	1	2,581	0,147	0,244

When testing the main effect of load for differences in displacement collapsed across groups (i.e., regardless of the type of abutment), a statistically significant difference in micromovements was found for U and V directions. The results of the within subjects effects for the three directions are summarized in table V.

Table V – Test of within-subjects effects: main effect of load for differences in micromovements across groups in the directions U, V and W. df- degrees of freedom; F- ANOVA test value.

	df	F	p	Partial Eta Squared
U	1,075	89,617	0,000	0,918
V	1,048	32,258	0,000	0,801
W	1,809	2,225	0,147	0,218

To determine if there were differences in micromovements between the two groups (anti-rotational and rotational abutments) when loaded at 50, 100, 150 and 200N an independent samples t-test was run.

Values of micromovements were normally distributed for all loads and displacement directions (U, V, W), as assessed by Shapiro-Wilks test ($p>0,05$). Homogeneity at variances, evaluated by Levenne's test for equality of variances was only violated for V displacement at 150 and 200N ($p=0,024$ and $p=0,011$ respectively).

For all directions and loads, no statistically significant differences were found between the two groups. The results are summarized in Table VI.

Table VI – Comparison of means of Rotational and Anti-Rotational abutments micromovements measured for each direction when subjected to loads of 50, 100, 150 and 200N. df: Degrees of Freedom; S.E.: Standard Error of difference; 95% C.I.: 95% confidence interval of difference.

		t-test for Equality of Means						
		T	Df	P	Mean Difference	S.E.	95% C.I.	
							Lower	Upper
maxU_50	Equal variances assumed	-1,258	8	,244	-,031	,024	-,087	,026
maxV_50	Equal variances assumed	-,525	8	,614	-,015	,028	-,080	,050
maxW_50	Equal variances assumed	1,353	8	,213	,063	,047	-,044	,171
maxU_100	Equal variances assumed	-,828	8	,432	-,027	,033	-,104	,049
maxV_100	Equal variances assumed	-1,002	8	,346	-,042	,042	-,138	,054
maxW_100	Equal variances assumed	1,263	8	,242	,074	,059	-,061	,210
maxU_150	Equal variances assumed	,014	8	,989	,001	,043	-,098	,100
maxV_150	Equal variances not assumed	-1,252	4,963	,266	-,073	,059	-,224	,078
maxW_150	Equal variances assumed	1,453	8	,184	,082	,056	-,048	,212
maxU_200	Equal variances assumed	,603	8	,563	,032	,053	-,090	,154
maxV_200	Equal variances not assumed	-1,494	4,600	,200	-,112	,075	-,310	,086
maxW_200	Equal variances assumed	2,220	8	,057	,122	,055	-,005	,248

4. Discussion

The first anti-rotational abutment system was the Branemark external hex. Originally designed solely to allow the engagement of a driver to seat the implant, it was ultimately adapted to prevent the rotation of abutments placed on the implant body[9]. However the significant complications that occur with this external connection like abutment screw loosening, rotational misfit at implant-abutment interface and microbial penetration have led to modification of the external hexagon and the development of the internal implant-abutment connections[53].

A systematic review showed a superiority of the internal connections relative to the external ones under the mechanical and prosthetic point of view, being cone morse the main highlight[49] since these provide such a perfect fixture-abutment fit to prevent bacterial penetration and mechanical complications[54]. Moreover, conical connections have a more central interface to implant platform, compared to external hexagon connections where peri-implant tissues are much closer[6, 55].

Those internal connections have been introduced to lower or eliminate the mechanical complications and stress transferred to the crestal bone occurred with the external connections[46, 56-57]. A primary question is whether or not this may be true for all internal connection systems[58] since, unlike the external hexagon connection, the internal connection configurations adopted by different companies are not alike. When analyzing the implant-abutment coupling of internal connecting systems, many differences have been described[58-62]:

• decreased gap between the abutment's surface and the internal walls of the implant fixture (no friction vs. Morse taper),
• depth of penetration of the abutment in the fixture,
• presence of anti-rotational interlocking,
• number and shape of anti-rotational or guiding grooves (hexagon, trilobe, spline, etc.),
• abutment diameter at the platform level (matched vs. narrower, to generate a platform shift or switch),
• abutment screw dimension and material,
• screw preload,
• abutment materials allowed (titanium, precious metal alloys, full zirconia, zirconia with metal inserts).

These differences might have profound impact on the clinical procedures and protocols, chair-time dedicated to the patient, number of appointments, laboratory and component costs, maintenance intervals, and incidence of complications. Therefore, the clinician has to analyze the different biomechanical features and understand their implications to make a rational choice between an external and an internal connection system[63].

The aspect which was investigated by this study was related with the presence or not of the anti-rotational interlocking and its correlation to the micromovements between the implant and the abutment.

In a previous study, done in 2012, at this University with the same protocol but using different implants (Cone Essential® [Klocner®] and Seven and C1[Mis®] implants) and abutments samples (including octagone, hexagonal internal connection and conical internal connection abutments) there were unexpected results demonstrating that the major micromovements occurred in the samples with conical internal connection (MIS®).

As the results aren't in accordance with the literature, where the majority of the studies shows the opposite with the conical connection suffering the less micromovements, and taking into account that the geometrical and characteristics of the implant-abutment connection are involved in the mechanical behavior, it came to the point to repeat the sample of the internal conical connection (MIS®) with anti-rotational abutments but this time to compare with rotational abutment to see if there was different results.

Rotational position stability of implant-abutment connection with different positional index designs has been investigated[9, 45]. The results indicate that the rotational freedom of different positional indices of the second and third generation is similar to that of hexagonal indices of the first generation [45]. Theoretical calculations show that the position stability depends on the geometric design of the index and the manufacturing tolerances[64].

The results of this study didn't show a significant difference between rotational and anti-rotational conical connection abutments, meaning that for this implant system there might be no difference in using a rotational or an anti-rotational abutment depending on the rehabilitation alternative.

Although no significant differences were found, the anti-rotational abutment revealed better performance for the U displacements up to 150N. From this point the displacement occurring in the anti-rotational abutment was clearly higher than the rotational one. Also, the rotational abutment revealed a better performance concerning vertical movements (V) particularly at higher loads as demonstrated by the spreading of lines in the profile plot (Graphic 4b). Concerning the W direction, the anti-rotational abutment showed a global better performance. The negative values found for the rotational abutment in this case could be due to freedom of rotation within the connection, resulting in displacement of the abutment towards the cameras. The null values associated to the anti-rotational abutments for all loads could mean very low rotational freedom of this type of abutments.

Even though there were no significant differences between the groups, both presented high values of micromovements when subjected to loading. The reason for these inflated values might be also related to the thickness of the implant walls in the internal conical connection that may be less resistant to the loads applied during the study. It is possible that some wall deformation occurs and this way allowing higher micromovement of the abutment. However, we can't extrapolate directly this information because the investigation was about micromovements and we didn't assess deformation.

A point that has to be taken in consideration is the fact that this study doesn't use crowns so the load is applied directly over the abutment. This limitation makes it more difficult to transpose these results to a normal clinical situation.

Also, another limitation is the rigid body motion, because there are many components that have to be eliminated due to the resilience of the surrounding materials when a force is applied over an object. With the elimination of those surrounding components we eliminated errors that could be induced.

Although at present conical connections are best performing from a biological and mechanical point of view, thanks to their implant-abutment better fitting, the ideal implant connection, able to zero down the risk of bacterial penetration, hasn't been implemented yet [65].

5. Conclusion

Within the limitations of this *in vitro* study the following conclusions can be drawn:

1. There is no significant difference in the behavior of an abutment with rotational or anti-rotational connection when it comes to internal conical connection from MIS®.

2. Even though there is no significant difference in the behavior of both groups, the anti-rotational abutment showed lower values of micromovements in the U and W directions. Attention should be paid to the vertical micromovements in the anti-rotational abutment.

6. Acknowledgments

To Professor Fernando Guerra and Dr. Salomão Rocha for their support and incentive in the achievement of this work. To Dr. Nuno Calha for his availability and encouragement in the concretion of the tests. To Dr. Ana Lúcia Messias for all the support, time spent and help in the statistical analysis. To Dr. Rui Isidro for all the help given. To Mis® for all the material provided to the study. To my family and friends for all the support and encouragement to accomplish this work.

References

1. Albrektsson T. A multicenter report on osseointegrated oral implants. J Prosthet Dent 1988;60(1):75-84.
2. Broggini N ML, Hermann JS, et al. Persistent acute inflammation at the implant-abutment interface. J Dent Res 2003;82:232-37.
3. Lekholm U, Gunne J, Henry P, Higuchi K, Linden U, Bergstrom C, et al. Survival of the Branemark implant in partially edentulous jaws: a 10-year prospective multicenter study. Int J Oral Maxillofac Implants 1999;14(5):639-45.
4. Pjetursson BE, Bragger U, Lang NP, Zwahlen M. Comparison of survival and complication rates of tooth-supported fixed dental prostheses (FDPs) and implant-supported FDPs and single crowns (SCs). Clin Oral Implants Res 2007;18 Suppl 3:97-113.
5. Jung RE, Pjetursson BE, Glauser R, Zembic A, Zwahlen M, Lang NP. A systematic review of the 5-year survival and complication rates of implant-supported single crowns. Clin Oral Implants Res 2008;19(2):119-30.
6. McGlumphy EA, Mendel DA, Holloway JA. Implant screw mechanics. Dent Clin North Am 1998;42(1):71-89.
7. Jorneus L, Jemt T, Carlsson L. Loads and designs of screw joints for single crowns supported by osseointegrated implants. Int J Oral Maxillofac Implants 1992;7(3):353-9.
8. Patterson EA, Johns RB. Theoretical analysis of the fatigue life of fixture screws in osseointegrated dental implants. Int J Oral Maxillofac Implants 1992;7(1):26-33.
9. Binon PP. The effect of implant/abutment hexagonal misfit on screw joint stability. Int J Prosthodont 1996;9(2):149-60.
10. Binon PP, Weir DJ, Marshall SJ. Surface analysis of an original Branemark implant and three related clones. Int J Oral Maxillofac Implants 1992;7(2):168-75.
11. al-Turki LE, Chai J, Lautenschlager EP, Hutten MC. Changes in prosthetic screw stability because of misfit of implant-supported prostheses. Int J Prosthodont 2002;15(1):38-42.
12. Khraisat A, Stegaroiu R, Nomura S, Miyakawa O. Fatigue resistance of two implant/abutment joint designs. J Prosthet Dent 2002;88(6):604-10.
13. Khraisat A, Hashimoto A, Nomura S, Miyakawa O. Effect of lateral cyclic loading on abutment screw loosening of an external hexagon implant system. J Prosthet Dent 2004;91(4):326-34.
14. Becker W, Becker BE, Newman MG, Nyman S. [Clinical and microbiological findings, that can cause failure of dental implants]. Quintessenz 1991;42(1):9-21.
15. Lang NP, Bragger U, Walther D, Beamer B, Kornman KS. Ligature-induced peri-implant infection in cynomolgus monkeys. I. Clinical and radiographic findings. Clin Oral Implants Res 1993;4(1):2-11.
16. Mombelli A, Marxer M, Gaberthuel T, Grunder U, Lang NP. The microbiota of osseointegrated implants in patients with a history of periodontal disease. J Clin Periodontol 1995;22(2):124-30.
17. Quirynen M, Op Heij DG, Adriansens A, Opdebeeck HM, van Steenberghe D. Periodontal health of orthodontically extruded impacted teeth. A split-mouth, long-term clinical evaluation. J Periodontol 2000;71(11):1708-14.
18. Quirynen M, Papaioannou W, van Steenberghe D. Intraoral transmission and the colonization of oral hard surfaces. J Periodontol 1996;67(10):986-93.
19. Tonetti MS. Risk factors for osseodisintegration. Periodontol 2000 1998;17:55-62.
20. Adell R, Lekholm U, Rockler B, Branemark PI, Lindhe J, Eriksson B, et al. Marginal tissue reactions at osseointegrated titanium fixtures (I). A 3-year longitudinal prospective study. Int J Oral Maxillofac Surg 1986;15(1):39-52.
21. Broggini N, McManus LM, Hermann JS, Medina RU, Oates TW, Schenk RK, et al. Persistent acute inflammation at the implant-abutment interface. J Dent Res 2003;82(3):232-7.
22. Bozkaya D, Muftu S. Mechanics of the tapered interference fit in dental implants. J Biomech 2003;36(11):1649-58.
23. Quirynen M, De Soete M, van Steenberghe D. Infectious risks for oral implants: a review of the literature. Clin Oral Implants Res 2002;13(1):1-19.

24. Hermann JS, Schoolfield JD, Schenk RK, Buser D, Cochran DL. Influence of the size of the microgap on crestal bone changes around titanium implants. A histometric evaluation of unloaded non-submerged implants in the canine mandible. J Periodontol 2001;72(10):1372-83.
25. King GN, Hermann JS, Schoolfield JD, Buser D, Cochran DL. Influence of the size of the microgap on crestal bone levels in non-submerged dental implants: a radiographic study in the canine mandible. J Periodontol 2002;73(10):1111-7.
26. Piattelli A, Vrespa G, Petrone G, Iezzi G, Annibali S, Scarano A. Role of the microgap between implant and abutment: a retrospective histologic evaluation in monkeys. J Periodontol 2003;74(3):346-52.
27. Gross M, Abramovich I, Weiss EI. Microleakage at the abutment-implant interface of osseointegrated implants: a comparative study. Int J Oral Maxillofac Implants 1999;14(1):94-100.
28. Duarte AR, Rossetti PH, Rossetti LM, Torres SA, Bonachela WC. In vitro sealing ability of two materials at five different implant-abutment surfaces. J Periodontol 2006;77(11):1828-32.
29. do Nascimento C, Barbosa RE, Issa JP, Watanabe E, Ito IY, Albuquerque RF, Jr. Bacterial leakage along the implant-abutment interface of premachined or cast components. Int J Oral Maxillofac Surg 2008;37(2):177-80.
30. Piattelli A, Scarano A, Paolantonio M, Assenza B, Leghissa GC, Di Bonaventura G, et al. Fluids and microbial penetration in the internal part of cement-retained versus screw-retained implant-abutment connections. J Periodontol 2001;72(9):1146-50.
31. Barbosa RE, do Nascimento C, Issa JP, Watanabe E, Ito IY, de Albuquerque RF, Jr. Bacterial culture and DNA Checkerboard for the detection of internal contamination in dental implants. J Prosthodont 2009;18(5):376-81.
32. do Nascimento C, Barbosa RE, Issa JP, Watanabe E, Ito IY, de Albuquerque Junior RF. Use of checkerboard DNA-DNA hybridization to evaluate the internal contamination of dental implants and comparison of bacterial leakage with cast or pre-machined abutments. Clin Oral Implants Res 2009;20(6):571-7.
33. Aloise JP, Curcio R, Laporta MZ, Rossi L, da Silva AM, Rapoport A. Microbial leakage through the implant-abutment interface of Morse taper implants in vitro. Clin Oral Implants Res 2010;21(3):328-35.
34. Jansen VK, Conrads G, Richter EJ. Microbial leakage and marginal fit of the implant-abutment interface. Int J Oral Maxillofac Implants 1997;12(4):527-40.
35. Kitamura E, Stegaroiu R, Nomura S, Miyakawa O. Biomechanical aspects of marginal bone resorption around osseointegrated implants: considerations based on a three-dimensional finite element analysis. Clin Oral Implants Res 2004;15(4):401-12.
36. Steinebrunner L, Wolfart S, Bossmann K, Kern M. In vitro evaluation of bacterial leakage along the implant-abutment interface of different implant systems. Int J Oral Maxillofac Implants 2005;20(6):875-81.
37. Yuzugullu B, Avci M. The implant-abutment interface of alumina and zirconia abutments. Clin Implant Dent Relat Res 2008;10(2):113-21.
38. Cibirka RM, Nelson SK, Lang BR, Rueggeberg FA. Examination of the implant-abutment interface after fatigue testing. J Prosthet Dent 2001;85(3):268-75.
39. Binon PP, McHugh MJ. The effect of eliminating implant/abutment rotational misfit on screw joint stability. Int J Prosthodont 1996;9(6):511-9.
40. Norton MR. Assessment of cold welding properties of the internal conical interface of two commercially available implant systems. J Prosthet Dent 1999;81(2):159-66.
41. Nikolopoulou F. Saliva and dental implants. Implant Dent 2006;15(4):372-6.
42. Khraisat A, Abu-Hammad O, Al-Kayed AM, Dar-Odeh N. Stability of the implant/abutment joint in a single-tooth external-hexagon implant system: clinical and mechanical review. Clin Implant Dent Relat Res 2004;6(4):222-9.
43. Coelho AL, Suzuki M, Dibart S, N DAS, Coelho PG. Cross-sectional analysis of the implant-abutment interface. J Oral Rehabil 2007;34(7):508-16.
44. Kano SC, Binon PP, Curtis DA. A classification system to measure the implant-abutment microgap. Int J Oral Maxillofac Implants 2007;22(6):879-85.
45. Semper W, Heberer S, Mehrhof J, Schink T, Nelson K. Effects of repeated manual disassembly and reassembly on the positional stability of various implant-abutment complexes: an experimental study. Int J Oral Maxillofac Implants 2010;25(1):86-94.

46. Merz BR, Hunenbart S, Belser UC. Mechanics of the implant-abutment connection: an 8-degree taper compared to a butt joint connection. Int J Oral Maxillofac Implants 2000;15(4):519-26.
47. Harder S, Dimaczek B, Acil Y, Terheyden H, Freitag-Wolf S, Kern M. Molecular leakage at implant-abutment connection--in vitro investigation of tightness of internal conical implant-abutment connections against endotoxin penetration. Clin Oral Investig 2010;14(4):427-32.
48. Harder S, Quabius ES, Ossenkop L, Kern M. Assessment of lipopolysaccharide microleakage at conical implant-abutment connections. Clin Oral Investig 2012;16(5):1377-84.
49. Dias R HM, Padovan L. Conexões implante-abutment. Salusvita, Bauru 2009;28:277-88.
50. Morneburg TR, Proschel PA. In vivo forces on implants influenced by occlusal scheme and food consistency. Int J Prosthodont 2003;16(5):481-6.
51. Sutton A, Orteu, J., Schreier, H., editor. Image Correlation for Shape, Motion and Deformation Measurements: Basic Concepts,Theory and Applications. New York: Springer; 2009.
52. Siebert T CM. Application of high speed digital image correlation for vibration mode shape analysis. SEM Annual Conference. Indianopolis, Indiana, USA; 2010.
53. Muley N PD, Gupta V. Evolution of External and Internal Implant to Abutment Connection. Int J Oral Implantol Clin Res 2012;3:122-29.
54. Meleo D, Baggi L, Di Girolamo M, Di Carlo F, Pecci R, Bedini R. Fixture-abutment connection surface and micro-gap measurements by 3D micro-tomographic technique analysis. Ann Ist Super Sanita 2012;48(1):53-8.
55. Coelho PG, Sudack P, Suzuki M, Kurtz KS, Romanos GE, Silva NR. In vitro evaluation of the implant abutment connection sealing capability of different implant systems. J Oral Rehabil 2008;35(12):917-24.
56. Norton MR. An in vitro evaluation of the strength of an internal conical interface compared to a butt joint interface in implant design. Clin Oral Implants Res 1997;8(4):290-8.
57. Finger IM, Castellon P, Block M, Elian N. The evolution of external and internal implant/abutment connections. Pract Proced Aesthet Dent 2003;15(8):625-32; quiz 34.
58. Steinebrunner L, Wolfart S, Ludwig K, Kern M. Implant-abutment interface design affects fatigue and fracture strength of implants. Clin Oral Implants Res 2008;19(12):1276-84.
59. Wiskott HW, Jaquet R, Scherrer SS, Belser UC. Resistance of internal-connection implant connectors under rotational fatigue loading. Int J Oral Maxillofac Implants 2007;22(2):249-57.
60. Coppede AR, Bersani E, de Mattos Mda G, Rodrigues RC, Sartori IA, Ribeiro RF. Fracture resistance of the implant-abutment connection in implants with internal hex and internal conical connections under oblique compressive loading: an in vitro study. Int J Prosthodont 2009;22(3):283-6.
61. Bernardes SR, de Araujo CA, Neto AJ, Simamoto Junior P, das Neves FD. Photoelastic analysis of stress patterns from different implant-abutment interfaces. Int J Oral Maxillofac Implants 2009;24(5):781-9.
62. Tsuge T, Hagiwara Y. Influence of lateral-oblique cyclic loading on abutment screw loosening of internal and external hexagon implants. Dent Mater J 2009;28(4):373-81.
63. Gracis S, Michalakis K, Vigolo P, Vult von Steyern P, Zwahlen M, Sailer I. Internal vs. external connections for abutments/reconstructions: a systematic review. Clin Oral Implants Res 2012;23 Suppl 6:202-16.
64. Semper W, Kraft S, Kruger T, Nelson K. Theoretical optimum of implant positional index design. J Dent Res 2009;88(8):731-5.
65. Ricomini Filho AP, Fernandes FS, Straioto FG, da Silva WJ, Del Bel Cury AA. Preload loss and bacterial penetration on different implant-abutment connection systems. Braz Dent J 2010;21(2):123-9.

Appendix

Table III – The maximum micromovements values in millimeters obtain for each sample of group A and B when exposed to forces of 50, 100, 150, 200N, at angles of 30º relative to the implant axis. (According to recorded movements there are different values for: **U**: it refers to the lateral movement, from left to right, when negative values it refers to the left movement; **V**: it refers to the occluso-cervical movement, when values are negative it translates the deepening of the object; **w**: it refers to the antero-posterior movement, when the values are negative it translates the posterior movement).

	Micromovements at 50 N			Micromovements at 100 N			Micromovements at 150 N			Micromovements at 200 N		
	u	v	w	u	V	w	u	v	w	u	v	w
A_1	0,011	-0,021	0,036	0,046	-0,051	0,047	0,109	-0,096	0,072	0,180	-0,145	0,065
A_2	0,001	0,021	-0,083	0,025	-0,015	-0,094	0,087	-0,042	-0,103	0,155	-0,080	-0,011
A_3	0,049	-0,114	0,085	0,112	-0,212	0,078	0,204	-0,344	0,066	0,294	-0,470	0,044
A_4	0,056	-0,050	0,017	0,169	-0,139	0,018	0,299	-0,237	0,016	0,429	-0,334	0,022
A_5	0,072	-0,021	-0,057	0,125	-0,054	-0,094	0,197	-0,101	-0,078	0,266	-0,150	-0,098
B_1	0,102	-0,047	-0,048	0,157	-0,084	-0,066	0,224	-0,131	-0,073	0,302	-0,184	-0,087
B_2	0,042	0,017	-0,119	0,090	0,013	-0,166	0,147	-0,041	-0,176	0,211	-0,078	-0,207
B_3	0,129	-0,075	0,025	0,183	-0,108	0,018	0,232	-0,137	0,022	0,257	-0,153	-0,032
B_4	0,046	0,010	-0,166	0,101	-0,027	-0,213	0,154	-0,055	-0,196	0,218	-0,090	-0,248
B_5	0,022	-0,015	-0,010	0,083	-0,055	0,011	0,137	-0,088	-0,013	0,176	-0,115	-0,014

Graphic 1 – Distribution of the maximum displacement values in both groups for each load to the U direction.

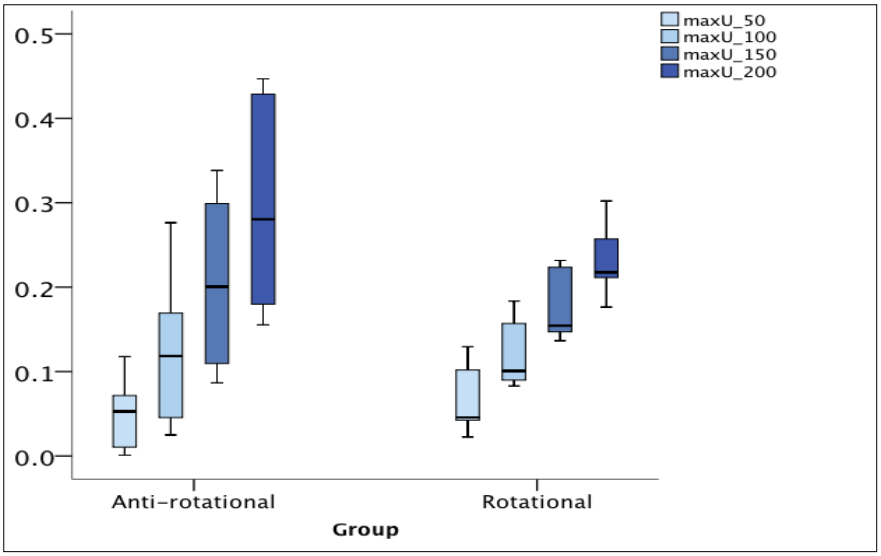

Graphic 2 – Distribution of the maximum displacement values in both groups for each load to the V direction.

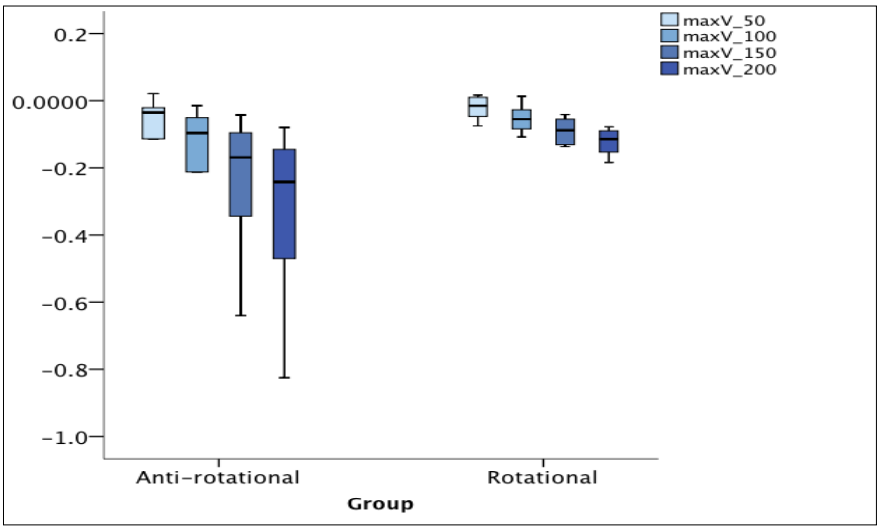

Graphics 3 – Distribution of the maximum displacement values in both groups for each load to the W direction.